Direct Measurement of Effective Magnetic Diffusivity in Turbulent Flow of Liquid Sodium

Peter Frick,* Vitaliy Noskov, Sergey Denisov, and Rodion Stepanov
Institute of Continuous Media Mechanics, Korolyov 1, Perm, 614013, Russia
(Received 13 July 2010; revised manuscript received 23 August 2010; published 27 October 2010)

The first direct measurements of effective magnetic diffusivity in turbulent flow of electroconductive fluids (the so-called β effect) under the magnetic Reynolds number $R_m \gg 1$ are reported. The measurements are performed in a nonstationary turbulent flow of liquid sodium, generated in a closed toroidal channel. The peak level of the Reynolds number reached $\mathrm{Re} \approx 3 \times 10^6$, which corresponds to the magnetic Reynolds number $R_m \approx 30$. The magnetic diffusivity of the liquid metal was determined by measuring the phase shift between the induced and the applied magnetic fields. The maximal deviation of magnetic diffusivity from its laminar value reaches about 50%.

DOI: 10.1103/PhysRevLett.105.184502 PACS numbers: 47.65.−d, 47.27.Jv

Small-scale turbulence plays a crucial role in cosmic magnetism, providing the small-scale (turbulent) magnetohydrodynamics (MHD) dynamo and contributing a lot to the dynamics of large-scale magnetic fields. The mean field (large-scale) dynamo equations are derived by applying the Reynolds approach to the MHD equations, and in the framework of the simplest case of homogeneous and isotropic (but mirror asymmetric) turbulence, they can be reduced to [1]

$$\partial_t \mathbf{B} = \nabla \times (\mathbf{U} \times \mathbf{B}) + \alpha \nabla \times \mathbf{B} + \eta \triangle \mathbf{B}, \quad \nabla \cdot \mathbf{B} = 0, \quad (1)$$

where $\mathbf{U}$ and $\mathbf{B}$ describe the mean (large-scale) velocity and magnetic fields, $\eta = \eta_0 + \beta$, η_0 is the Ohmic magnetic diffusivity, and α and β are the turbulent transport coefficients, describing the action of small-scale turbulent pulsations on the mean field dynamics (see e.g. [2]). Coefficient α describes the generation effects, and β describes the contribution of turbulence to the diffusion of the large-scale magnetic field. The knowledge of the magnetic turbulent transport coefficients α and β is basic for astrophysical and geophysical applications in dynamo theory [3].

Over the last decade, major efforts were directed toward the study of MHD dynamo in laboratory experiments (for a review, see [4]). The first-generation dynamo experiments were designed on the basis of strictly specified large-scale flow. The Riga dynamo is driven by the cylindrical screw flow [5], the Cadarache dynamo is based on a von Kármán flow between two counterrotating disks [6], and even the Karlsruhe dynamo, defined as a "two-scale" dynamo, is driven by a set of strictly prescribed helical jets inside 52 tubes [7]. In this sense, all laboratory dynamos can be classified as quasilaminar. In spite of that, the Reynolds numbers reached about 10^7 and the flows were fully turbulent in all experiments. Thus, the role of turbulence is reduced in these experiments to the enhancement of the diffusion of the magnetic field which, with a constant magnetic permeability, can be considered as an increase in the effective resistance of liquid metal. The growth of resistivity can be crucial for dynamo experiments because of the corresponding reduction in the magnetic Reynolds number. However, no direct measurement of the effective resistivity in dynamo facilities has been performed up to now. An indirect indication of the beta effect has been obtained in the Madison sodium facilities by comparing the measured magnetic field and the magnetic field simulated on the base of the measured mean velocity field [8]. An interesting scheme of eddy diffusivity estimation from hydromagnetic Taylor-Couette flow experiment was recently suggested in [9].

The direct measurements of β are impeded by the fact that the effect appears only under very large Reynolds numbers, when numerous side effects prevent the accurate isolation of the β effect. The first attempt of such measurements was done in a flow generated by a propeller in a vessel containing liquid sodium [10], though the authenticity of the obtained data is questionable both with respect to the level of the observed conductivity variations and the estimates of the measurement errors.

A promising method of designing high Reynolds number flows (although nonstationary) in the limited mass of liquids was proposed in [11], in which the flow was generated by the abrupt braking of a fast-rotating toroidal channel. Installation of diverters in the channel made it possible to create a toroidal screw flow of liquid gallium, in which, for the first time, the α effect was observed, defined by a joint action of the gradient of turbulent pulsations and large-scale vorticity [12]. The study of the dynamics of the nonstationary flow in a torus *without* diverters has shown that the development of the flow in the channel is characterized by a strong short-time burst of turbulent pulsations with a peak in the range on the order of 500–1000 Hz [13]. This burst of small-scale turbulence provides an opportunity to detect the increase in effective resistivity of liquid metal using the low frequency alternating magnetic field (~ 100 Hz). The idea of such an experiment has been realized in the nonstationary flow of liquid gallium. The toroidal channel produced from textolite made it possible to get magnetic Reynolds number less than unity [14].

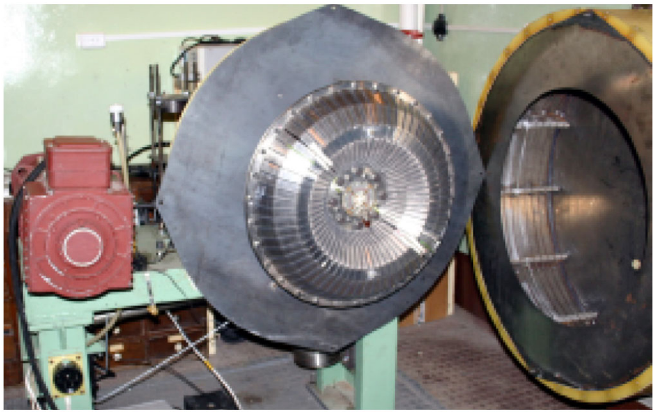

FIG. 1 (color online). Titanium channel and thermostatic cover.

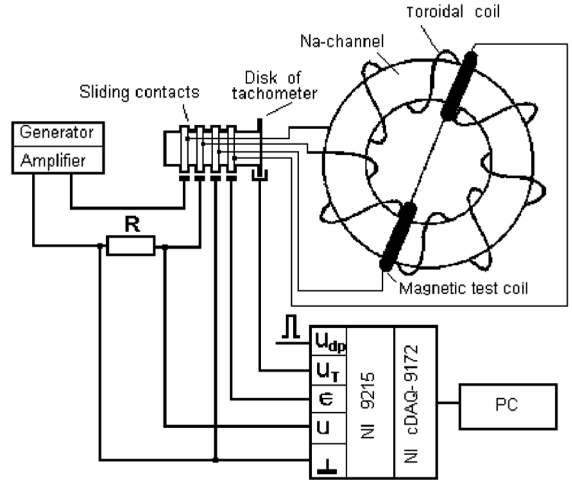

FIG. 2. Schematic circuit of the measuring system. U_{dp}, U_T, E, and U are the driving pulse, the tachometer signal, the electromotive force of the magnetic test coil, and the voltage, corresponding to the applied current.

In this paper we exploit a similar experimental scheme using a titanium toroidal channel of larger size, filled with liquid sodium, which allows us to increase the magnetic Reynolds number by 2 orders of magnitude.

The apparatus is an electromechanical construction mounted on a rigid frame, which is used as a support for a rotating toroidal channel (Fig. 1). The torus radius is $R = 0.18$ m; the radius of the channel cross section is $r = 0.08$ m. The channel was filled with sodium under the vacuum condition and was placed into the air thermostat. The channel temperature may be stabilized in the range (50–150) °C. The temperature sensor is mounted inside the channel and has good thermic contact with the sodium in both liquid and solid states.

The channel is fastened on the horizontal axis, which is also used for mounting a driving pulley, a system of sliding contacts, and a disk braking system. The frequency of the channel's rotation is up to 45 rps, and the flow in the channel is generated by abrupt braking—the braking time is no more than 0.3 s. The maximum velocity of the flow is reached after the channel is stopped and achieves about 70% of the linear velocity of the channel before braking. This means that the Reynolds number $\mathrm{Re} = Ur/\nu$ (ν is the kinematic viscosity of the liquid sodium) reaches, at maximum, the value $\mathrm{Re} \approx 3 \times 10^6$, which corresponds to the magnetic Reynolds number $R_m = Ur/\eta_0 \approx 30$. The schematic circuit is shown in Fig. 2. The "generator-amplifier" block creates, in the toroidal coil, a stabilized sinusoidal current with frequency $30 < \nu < 1000$ Hz, which produces an alternating toroidal magnetic field inside the channel. Besides the toroidal coil, two diametrically located magnetic test coils are wound around the channel.

The change in phase shift θ between the measured magnetic field and the alternating current in the toroidal coil is a value which can be treated as a measure of logarithmic changes of diffusivity of the sodium,

$$\Delta\theta \simeq C\rho^{-1}\Delta\rho = C\eta^{-1}\Delta\eta, \qquad (2)$$

where C is a dimensional coefficient which depends on the geometry and resistivity of the channel wall, and on the frequency of the applied magnetic field. The measuring system is completed with software based on wavelet analysis, which provides calculation of the time dependence of the phase shift after recording the signal. Wavelets are required because the variation of the phase shift occurs at times comparable with the oscillation period.

The measurement system has been tested and calibrated by measuring the dependence of the sodium resistivity on the temperature. The channel containing the sodium was cooled down from 105 °C to 80 °C. This range of temperature includes the sodium freezing point, which gives the best measure for calibration because the resistivity of the sodium decreases at that point by 31%, while the temperature remains constant. This excludes the influence of resistivity variation of titanium, coils, etc. Figure 3 shows the results of phase shift measurements performed at frequency $\nu = 97$ Hz, together with results of numerical simulations. For this frequency, the skin layer thickness

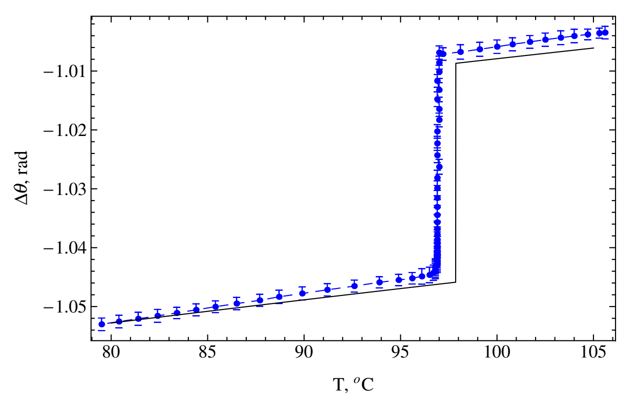

FIG. 3 (color online). Phase shift versus sodium temperature at frequency $\nu = 97$ Hz: experiment (points) and simulations (solid line).

of titanium is about 44 mm (the mean thickness of the titanium wall is about 10 mm) and the skin layer thickness of sodium is about 16 mm.

The theoretical phase shift in the skin layer of an infinite cylindrical solenoid, which includes a titanium cylinder tube with sodium, fits the experimental points well, and allows us to define the factor of proportionality in relation (2) for each applied frequency. For the case $\nu = 97$ Hz, shown in Fig. 3, $C = 102 \pm 3$ mrad. For verification of the method, an alternative approach of evaluating the sodium resistivity was used, based on the equivalent electrotechnical schematic of the transformer with the short-circuited secondary winding, which gave close results.

All dynamical experiments concerning the turbulent flow of liquid sodium were performed under the fixed temperature $T = (102 \pm 1)\,^\circ$C. The estimation of sodium heating due to energy dissipation in decaying turbulent flow at the highest rotational velocity $f = 50$ rps (considering that its entire kinetic energy will dissipate in the heat) gives $\Delta T \approx 0,\ 8\,^\circ$C, which corresponds to variations of resistivity of less than 0.5%.

Results and summary.—The rotational velocity Ω varied from 10 to 45 rps with a step of 5 rps. Measurements for all Ω were performed using three different frequencies ν (53, 66, and 97 Hz). The evolution of the phase shift, measured at frequency $\nu = 97$ Hz for different velocities of the channel rotation Ω, is shown in Fig. 4. Each curve is the result of averaging over 10 realizations. The end of braking is defined as the reference time point ($t = 0$). One can see that braking generates the turbulent flow, the maximal intensity of which coincides with the end of braking. At this moment the phase shift also reaches its maximum. Later on, turbulent pulsations rapidly decay and the phase shift reduces to zero.

As shown in the inset of Fig. 4, the phase shift decays exponentially, unlike the usual free decay of developed turbulence that involves power laws. The turbulent boundary layer in the nonstationary toroidal flow is developed in a very specific way. This was found in studies of the dynamics of a similar flow of liquid gallium, which have shown that the decay of the mean energy of the turbulent flow in the toroidal channel follows the t^{-2} law, while the burst of turbulent pulsations attends the flow formation and deceases abruptly [13]. This is an additional argument in favor of the small-scale turbulence (as opposed to the mean flow dynamics) as the reason for the phase shift measured.

We have examined the flow across a broad range of frequencies, $31 \le \nu \le 516$ Hz (the skin layer thickness then varies from 29 to 7 mm). Figure 5 shows the phase shift for various frequencies, confirming that the turbulent diffusivity is related to the turbulent intensity, which grows with distance from the channel wall towards its axis—at low frequencies, the contribution of the near-axis region is larger, so that the β effect is more pronounced. At its highest frequency, the measuring system samples only the boundary layer, which develops first: for $\nu = 516$ Hz, the phase shift reaches a maximum at $t = -0.15$ s, while for $\nu = 31$ Hz, the maximum appears only at $t = 0.4$ s.

In Fig. 6 we show how the observed β effect depends on the intensity of the mean flow (on the Reynolds number, which is defined by the channel rotation rate before braking). First, we show [Fig. 6(a)] the maximal deviation of effective magnetic diffusivity, which corresponds to the end of braking, from the basic value. Measurements are taken using three frequencies: $\nu = 53$, 66, and 97 Hz. Changing frequency, we vary the depth of penetration of the magnetic field into the turbulent flow. As the frequency is lowered, the thicker the skin layer becomes, the more pronounced the observed β effect is. The maximal value (for $\Omega = 45$ rps and $\nu = 53$ Hz) exceeds 50%. At low rotation rates the effect increases monotonically, in a similar manner for all frequencies; however, with $\Omega > 30$ rps, the monotonicity disappears and the curves develop in disorder. Examining individual curves in Fig. 4, it is possible to see that, with high rotational speeds, the structure of the curve near the maximum becomes very complex. However, curves evolve quite similarly without any

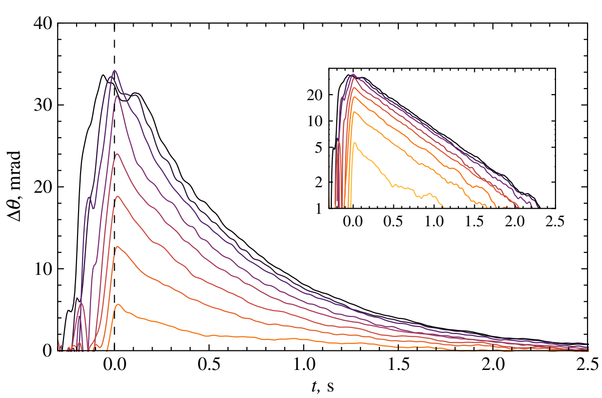

FIG. 4 (color online). Phase shift variations for the channel rotation rate $\Omega = 10, 15, \ldots, 40, 45$ rps (from bottom to top) in linear and lin-log (inset) scales. $\nu = 97$ Hz.

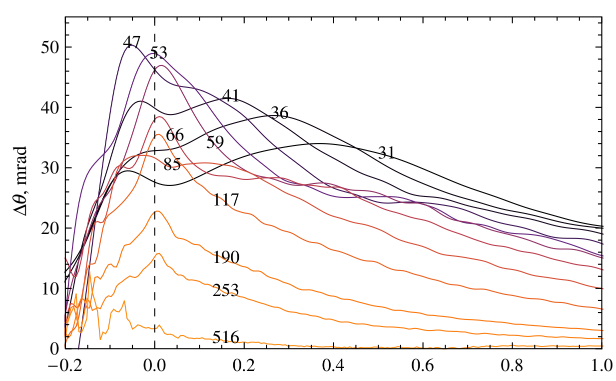

FIG. 5 (color online). Phase shift variations for the channel rotation rate $\Omega = 40$ rps and different frequency ν, shown near each curve.

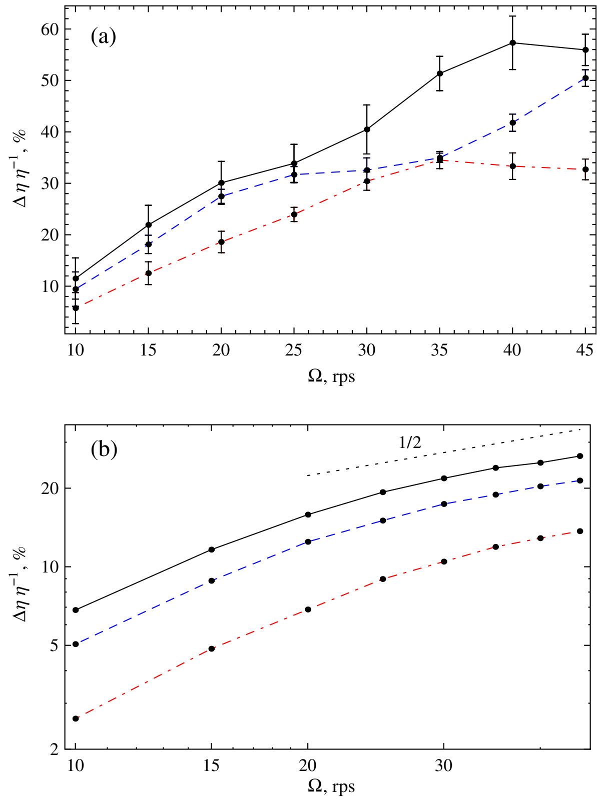

FIG. 6 (color online). Relative increase of magnetic diffusivity (percentage) versus the channel rotation rate Ω at the end of braking (a) and at 0.7 s (b): $\nu = 53$ Hz (solid, black line), $\nu = 66$ Hz (dashed, blue line), and $\nu = 97$ Hz (dash-dot, red line). Panel (b) is shown in logarithmic scale; dots show the power law "1/2."

deviation after $t \approx 0.2$. We show in the lower panel of Fig. 6 the deviation of effective magnetic diffusivity at $t = 0.7$ s. Then, all three curves show a similar monotonic increase of the β effect. Shown in logarithmic scales, they display a tendency toward a power law $\Delta\eta \sim \Omega^{1/2}$ at high rotational velocity.

So, the measurement of electric conductivity in the nonstationary, fully developed, turbulent ($\mathrm{Re} \lesssim 3 \times 10^6$) flow of liquid sodium in a closed channel shows that the effective magnetic diffusivity essentially increases with the Reynolds number. For the maximal rotation rate $\Omega = 45$ rps, which corresponds to $R_m \approx 30$, the maximal deviation of magnetic diffusivity reaches about 50%. Experiments with liquid gallium at low magnetic Reynolds number ($R_m < 1$) revealed a quadratic-like dependence $\beta \sim \mathrm{Rm}^2$ [14], which corresponds to general conceptions of the beta effect for low R_m. Our results show that the quadratic law does not hold at moderate R_m. Note that the turbulent viscosity in *stationary* pipe flows at high Re increases as $\nu_t \sim \mathrm{Re}^{1/2}$ [15], and our results show, at the highest Reynolds numbers, a tendency to the same power law. One should apply the obtained dependence to the case of stationary pipe flow, or to homogeneous turbulence, with great caution. However, in view of the fact that the problem of measuring the examined characteristic in real flows is very complicated, and that experimental data are completely absent, measurement of the effective magnetic diffusivity in the turbulent medium, even in one particular case, is an important step toward the experimental substantiation of general MHD-dynamo conceptions.

This work was supported by ISTC Project No. 3726 and RFBR-CNRS Grant No. 07-01-92160.

*frick@icmm.ru

[1] M. Steenbeck, F. Krause, and K. Rädler, Z. Naturforsch. A **21**, 369 (1966).
[2] H. K. Moffatt, *Magnetic Field Generation in Electrically Conducting Fluids* (Cambridge University Press, Cambridge, England, 1978); F. Krause and K.-H. Rädler, *Mean-field Magnetohydrodynamics and Dynamo Theory* (Pergamon Press, New York, 1980).
[3] Y. B. Zeldovich, A. A. Ruzmaikin, and D. D. Sokoloff, *Magnetic Fields in Astrophysics* (Gordon and Breach, New York, 1983).
[4] F. Stefani, A. Gailitis, and G. Gerbeth, Z. Angew. Math. Mech. **88**, 930 (2008).
[5] A. Gailitis, O. Lielausis, S. Dement'ev, E. Platacis, A. Cifersons, G. Gerbeth, T. Gundrum, F. Stefani, M. Christen, and H. Hänel *et al.*, Phys. Rev. Lett. **84**, 4365 (2000).
[6] R. Monchaux, M. Berhanu, M. Bourgoin, M. Moulin, P. Odier, J. Pinton, R. Volk, S. Fauve, N. Mordant, and F. Pétrélis *et al.*, Phys. Rev. Lett. **98**, 044502 (2007).
[7] R. Stieglitz and U. Müller, Phys. Fluids **13**, 561 (2001).
[8] E. J. Spence, M. D. Nornberg, C. M. Jacobson, C. A. Parada, N. Z. Taylor, R. D. Kendrick, and C. B. Forest, Phys. Rev. Lett. **98**, 164503 (2007).
[9] M. Gellert and G. Rüdiger, Phys. Rev. E **80**, 046314 (2009).
[10] A. B. Reighard and M. R. Brown, Phys. Rev. Lett. **86**, 2794 (2001).
[11] P. Frick, V. Noskov, S. Denisov, S. Khripchenko, D. Sokoloff, R. Stepanov, and A. Sukhanovsky, Magnetohydrodynamics **38**, 143 (2002).
[12] R. Stepanov, R. Volk, S. Denisov, P. Frick, V. Noskov, and J.-F. Pinton, Phys. Rev. E **73**, 046310 (2006).
[13] V. Noskov, R. Stepanov, S. Denisov, P. Frick, G. Verhille, N. Plihon, and J. Pinton, Phys. Fluids **21**, 045108 (2009).
[14] S. A. Denisov, V. I. Noskov, R. A. Stepanov, and P. G. Frick, JETP Lett. **88**, 167 (2008).
[15] H. Schlichting, *Grenzschicht-Theorie* (G. Braun, Karlsruhe, 1954).